Targeting BRAF[V600E] with PLX4720 Displays Potent Antimigratory and Anti-invasive Activity in Preclinical Models of Human Thyroid Cancer

CARMELO NUCERA,[a,e] MATTHEW A. NEHS,[a] SUSHRUTA S. NAGARKATTI,[a] PETER M. SADOW,[b]
MICHAL MEKEL,[a] ANDREW H. FISCHER,[c] PAUL S. LIN,[d] GIDEON E. BOLLAG,[d] JACK LAWLER,[e]
RICHARD A. HODIN,[a] SAREH PARANGI[a]

[a]Thyroid Cancer Research Laboratory, Endocrine Surgery Unit, and [b]Department of Pathology, Massachusetts General Hospital, Harvard Medical School, Boston, Massachusetts, USA; [c]Department of Pathology, University of Massachusetts, Worcester, Massachusetts, USA; [d]Plexxikon Inc., Berkeley, California, USA; [e]Division of Cancer Biology and Angiogenesis, Department of Pathology, Beth Israel Deaconess Medical Center, Harvard Medical School, Boston, Massachusetts, USA

ABSTRACT

Purpose. B-Raf[V600E] may play a role in the progression from papillary thyroid cancer to anaplastic thyroid cancer (ATC). We tested the effects of a highly selective B-Raf[V600E] inhibitor, PLX4720, on proliferation, migration, and invasion both in human thyroid cancer cell lines (8505c[B-RafV600E] and TPC-1[RET/PTC-1 and wild-type B-Raf]) and in primary human normal thyroid (NT) follicular cells engineered with or without B-Raf[V600E].

Experimental Design. Large-scale genotyping analysis by mass spectrometry was performed in order to analyze >900 gene mutations. Cell proliferation and migra-

tion/invasion were performed upon PLX4720 treatment in 8505c, TPC-1, and NT cells. Orthotopic implantation of either 8505c or TPC-1 cells into the thyroid of severe combined immunodeficient mice was performed. Gene validations were performed by quantitative polymerase chain reaction and immunohistochemistry.

Results. We found that PLX4720 reduced in vitro cell proliferation and migration and invasion of 8505c cells, causing early downregulation of genes involved in tumor progression. PLX4720-treated NT cells overexpressing B-Raf[V600E] (heterozygous wild-type B-Raf/

B-Raf^{V600E}) showed significantly lower cell proliferation, migration, and invasion. PLX4720 treatment did not block cell invasion in TPC-1 cells with wild-type B-Raf, which showed very low and delayed in vivo tumor growth. In vivo, PLX4720 treatment of 8505c orthotopic thyroid tumors inhibited tumor aggressiveness and significantly upregulated the thyroid differentiation markers thyroid transcription factor 1 and paired box gene 8.

Conclusions. Here, we have shown that PLX4720 preferentially inhibits migration and invasion of B-Raf^{V600E} thyroid cancer cells and tumor aggressiveness. Normal thyroid cells were generated to be heterozygous for wild-type B-Raf/B-Raf^{V600E}, mimicking the condition found in most human thyroid cancers. PLX4720 was effective in reducing cell proliferation, migration, and invasion in this heterozygous model. PLX4720 therapy should be tested and considered for a phase I study for the treatment of patients with B-Raf^{V600E} ATC. *The Oncologist* 2011;16:296–309

INTRODUCTION

The incidence of well-differentiated thyroid cancers has been increasing [1]. The majority of patients with these tumors have a low risk for recurrence or death with standard therapy (surgery, radioiodine, and thyroid-stimulating hormone [TSH] suppression). However, a subset of patients with aggressive thyroid cancer, especially anaplastic thyroid carcinoma (ATC), present with locally advanced disease that recurs and metastasizes [2]. Mutations in key regulatory genes are likely to play an important role. Mutations known to be important in papillary thyroid cancers (PTCs) include: *RET/PTC* translocation (10%–50% of PTCs) [3, 4], *Ras* mutations (about 12% of PTCs) [5], and *B-Raf^{V600E}* mutations (29%–83% of PTCs) [6, 7]. *B-Raf^{V600E}* is the second most common somatic mutation in human cancer, with a frequency of approximately 8% [8]. The B-Raf^{V600E} protein (valine-to-glutamate, position 600) results from a transversion in the gene (T1799A) and results in increased mitogen-activated protein kinase (e.g., mitogen-activated protein kinase/extracellular signal–related kinase kinase [MEK]-1/MEK-2, extracellular signal–related kinase [ERK]-1/ERK-2) activity [8, 12]. When PTC and ATC occur together in the same thyroid malignant lesion, they generally share the *B-Raf^{V600E}* mutation, implying that many ATCs are derived from malignant degeneration of pre-existing well-differentiated PTCs [13]. Our study focuses on further elucidating the role of this mutation in aggressive thyroid cancers.

PLX4720 (7-azaindole derivative) is a selective small molecule inhibitor of B-Raf^{V600E} [14]. PLX4720 was designed to block the ATP-binding site of oncogenic B-Raf^{V600E} [14]. PLX4720 binds selectively to the active B-Raf^{V600E} protein conformation. Consistent with the high degree of selectivity, PLX4720 inhibits B-Raf^{V600E} kinase activity both in vitro and in vivo in melanoma and colorectal tumor cell models [14].

We performed in vitro testing of PLX4720 on human thyroid cancer cell lines harboring the *B-Raf^{V600E}* mutation or the *RET/PTC-1* translocation (with wild-type [wt] *B-Raf* in both alleles) and on primary human normal thyroid (NT) follicular cells engineered to express B-Raf^{V600E}. We furthermore used an orthotopic mouse model of ATC harboring *B-Raf^{V600E}* to test in detail the in vivo activity of PLX4720 on tumor aggressiveness using an early intervention model.

MATERIALS AND METHODS

Antibodies

Antibodies for Western blot (WB) and immunohistochemistry (IHC) are reported in the supplemental online data.

PLX4720 Preparation

PLX4720 was dissolved in dimethyl sulfoxide (DMSO) at 1 μM or 10 μM for in vitro assays. For the in vivo preparation, PLX4720 was dissolved in DMSO (120 mg/ml) and then suspended in a 1% solution of carboxymethycellulose (Sigma, St. Louis).

Human Thyroid Cancer Cell Lines and NT Cells

We used the TPC-1 cell line (human PTC, *RET/PTC-1*/wt for *B-Raf*), provided by Dr. F. Frasca (University of Catania, Catania, Italy), and the 8505c cell line (human ATC harboring *B-Raf^{V600E}*), purchased from DSMZ (German collection of microorganisms and cell culture) [15]. NT cells were obtained according to Fischer et al. [16]. All in vitro assays were performed by growing these cell lines with the specific growth medium supplemented with 1% fetal bovine serum. More details are reported in the supplemental online data.

Cell Transfections for Retrovirus Production

Sixty-millimeter plates of HEK 293T cells (5×10^5) were transfected using Fugene-6 (Roche, Indianapolis) in OptiMEM (Invitrogen, Carlsbad, CA) for 48 hours.

B-Raf^{V600E} Transduction in NT Cells

B-Raf^{V600E}-pBABE-puro and pBABE-puro (empty vector) retroviral constructs were provided by Dr. W.C. Hahn (Dana

Farber Cancer Institute, Harvard Medical School, Boston, MA) [17] and used for *B-Raf*^{V600E} overexpression (transduction) studies in NT cells (passage 0). For analysis, cells were pelleted then processed according to Nucera et al. [18]. More details are reported in the supplemental online data.

WB Analysis
WB assays and band densitometry were performed according to a standard procedure [19].

Cell Cycle Analysis, Bromodeoxyuridine Assay, and Apoptosis Assay
8505c, TPC-1, and NT cells were seeded at 3×10^5 cells/10-cm dish. After 72 hours of treatment with PLX4720 (1 μM or 10 μM) or vehicle, bromodeoxyuridine (BrdU, 10 μM) (Upstate Cell Signaling Solutions, Temecula, CA) was added for 1 hour. The cell cycle analysis, BrdU assay, and apoptosis assay were performed in triplicate according to Nucera et al. [19].

Migration and Invasion Assays
Migration and invasion assays were performed in triplicate using 8505c cells (8×10^3 cells/assay), TPC-1 cells (8×10^3 cells/assay), and NT cells (25×10^3 cells/assay) for 72 hours in culture. More details are reported in the supplemental online data.

Quantitative Multigene Profiling by Real-Time Reverse Transcriptase Polymerase Chain Reaction Analysis
Quantitative multigene and absolute real-time reverse transcriptase polymerase chain reaction (RT-PCR) were performed according to Shih and Smith [20] (supplemental online data and supplemental online Table 1).

Tumor Implantation
Animal work was performed in the animal facility at Massachusetts General Hospital (Boston, MA) in accordance with federal, local, and institutional guidelines. Orthotopic thyroid tumor implantation was done as previously described in severe combined immunodeficient (SCID) mice (Charles River Laboratories, Wilmington, MA) using 8505c cells (5×10^5) engineered with green fluorescent protein (GFP) [21] or TPC-1 cells (1×10^6). Given our early-intervention design, 1 week post–tumor implantation mice were treated with either PLX4720 (30 mg/kg per day, $n = 8$) by oral gavage (Plexxikon, Berkeley, CA) or vehicle ($n = 8$) once daily for 21 days. Weight was recorded weekly.

Tumor burden was evaluated weekly by palpation, and mice underwent necropsy 35 days after tumor implantation.

Tumor size was measured using an electronic caliper. Tumor volume was calculated as $(1/2) \times$ length $\times$ width $\times$ height. Tumors, regional lymph nodes, and lungs were also analyzed by histology.

In Vivo and Ex Vivo Bioimaging, Histological, and IHC Analysis of Orthotopic Thyroid Tumors
The computed tomography, multispectral fluorescence scanner (CRi Maestro 500, CRi Inc., Woburn, MA), histopathology, and IHC are described in the supplemental online data.

Scoring for Metastases
Metastases were counted and averaged at 40$\times$ using hematoxylin and eosin–stained, formalin-fixed sections of lymph nodes and lungs.

Mass Spectrometric Genotyping
Genomic DNA from thyroid cancer lines was purified and subjected to mass spectrometric genotyping as described previously [22]. The *RET/PTC-1* analysis was performed according to Puxeddu et al. [23].

Statistical Analysis
Statistical analyses were performed using Microsoft Excel with Student's *t*-test and the χ^2 test. *p*-values <.05 were considered significant (*$p < .05$, **$p < .01$, ***$p < .001$). The data represent the average $\pm$ standard deviation or, in the case of real-time RT-PCR or mice experiments, mean $\pm$ standard error of the mean.

RESULTS

PLX4720 Downregulates ERK-1/ERK-2 Phosphorylation and Inhibits Migration and Invasion in 8505c Cells Harboring *B-Raf*^{V600E}
For our in vitro studies, we used 8505c, an aggressive and authentic [24] human thyroid carcinoma cell line that we have shown to be tumorigenic and metastatic in vivo [21] and to harbor the V600E mutation and *TP53* R248G mutation (by mass spectrometric genotyping) (Fig. 1A); 8505c cells were found to be negative for other mutations (e.g., H-, N-, and K-*RAS* mutations, etc.). Treatment with 1 μM PLX4720 resulted in a >90% reduction in phospho-ERK-1/ERK-2 protein levels after 1 hour (Fig. 1B) with no significant difference in cell proliferation (BrdU uptake) even after 72 hours (control versus PLX4720 treatment, 22.6% $\pm$ 3.3% versus 18.4% $\pm$ 1.4%; $p = 0.1$) (Fig. 2A, 2B, 2D), whereas treating 8505c cells with 10 μM PLX4720 for 1 hour or 72 hours reduced phospho-ERK-1/ERK-2 (Fig. 1B, 1C), reduced BrdU uptake (19.8% $\pm$ 0.8% versus 3.7% $\pm$ 1.2% in control versus
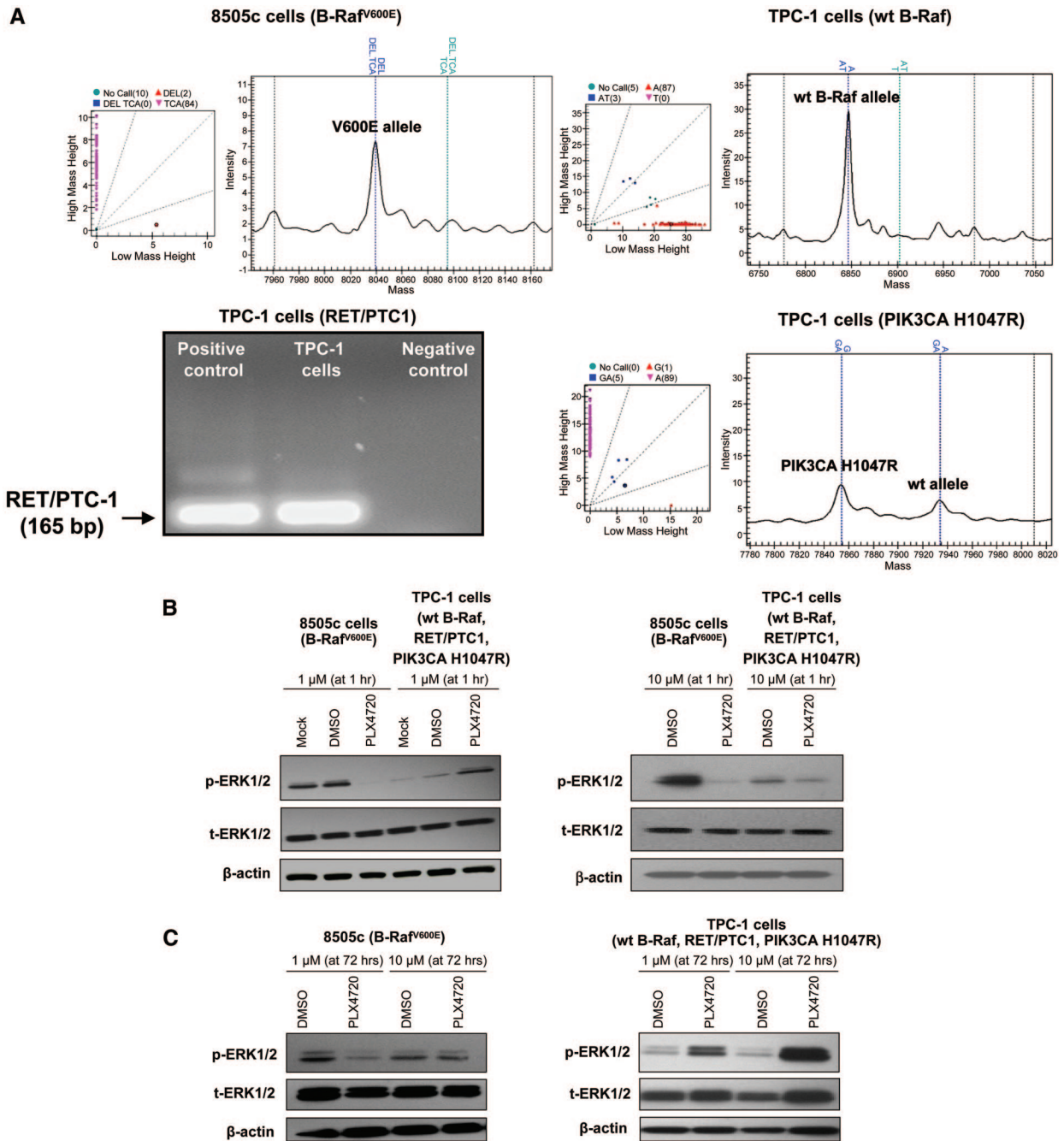
A

Figure 1. p-ERK-1/ERK-2 expression in thyroid cancer cells. **(A):** *B-Raf*[V600E] mutation in 8505c cells; TPC-1 cells have wt *B-Raf* and harbor the *PIK3CA* H1047R mutation and *RET/PTC-1* translocation. **(B):** One hour of 1 μM PLX4720 treatment resulted in lower p-ERK-1/ERK-2 levels (by Western blotting) in 8505c cells, but higher levels in TPC-1 cells. p-ERK-1/ERK-2 levels were lower in 8505c cells and TPC-1 cells with 10 μM PLX4720. **(C):** 72 hours of PLX4720 treatment resulted in lower p-ERK-1/ERK-2 levels in 8505c cells and higher levels in TPC-1 cells.

Abbreviations: DMSO, dimethyl sulfoxide; ERK, extracellular signal–related kinase; p, phosphorylated; wt, wild-type.

PLX4720, respectively; $p = .001$), reduced the S-phase cell fraction (Fig. 2A, 2B), and caused G_1 arrest (38.9% ± 1.8% versus 56.4% ± 1.9% in control versus PLX4720, respectively; $p < .001$) (Fig. 2D). PLX4720 treatment (1 μM or 10 μM) did not lead to apoptosis (ab-

sence of sub-G_1 cell population) according to the flow cytometric analysis (Fig. 2D).

Recently, it was demonstrated that PLX4720 induces activation of C-Raf [25]. We analyzed C-Raf protein levels and did not find a significant difference after 1 hour
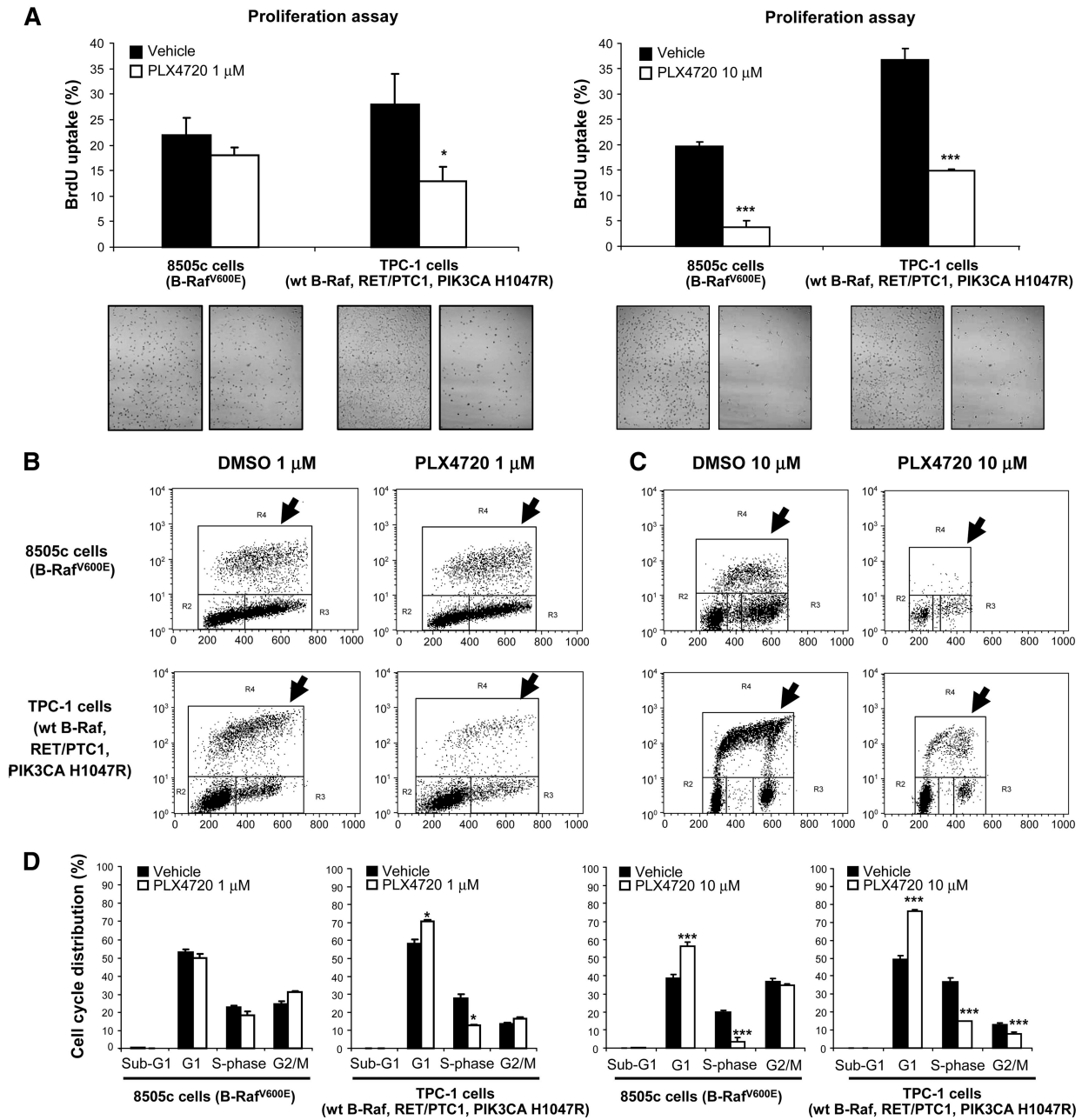
Figure 2. PLX4720 inhibits proliferation in thyroid cancer cells. **(A–C):** 1 μM PLX4720 reduced BrdU incorporation in TPC-1 cells (*p = .01); 10 μM PLX4720 reduced BrdU uptake in 8505c and TPC-1 cells (***p < .001). **(D):** 1 μM PLX4720 significantly reduced S-phase (*p = .01) and caused G$_1$ phase arrest (**p < .01) in TPC-1 cells and 10 μM PLX4720 reduced S-phase (***p < .001) and caused G$_1$ phase arrest (**p < .001) in both TPC-1 and 8505c cells.
Abbreviations: BrdU, bromodeoxyuridine; DMSO, dimethyl sulfoxide; wt, wild-type.

with PLX4720 treatment compared with controls (supplemental online Fig. 1A). Additionally, the Raf–ERK pathway can synergize with phosphoinositide 3-kinase (PI3K)/Akt–mediated signaling on specific biochemical effectors [26] and we wanted to see whether phospho-ERK-1/ERK-2 downregulation by PLX4720 could affect downstream targets such as Akt phosphorylation levels. We found no significant difference in phospho-Akt

ser473 protein levels in 8505c cells after 1 hour with PLX4720 treatment, compared with the control (supplemental online Fig. 1A).

We have previously shown an important role for *B-Raf*[V600E] in mediating migration and invasion of 8505c into Matrigel [19]. One micromolar PLX4720 reduced migration from 71.3 $\pm$ 1.5 cells/field to 35 $\pm$ 1 migrated cells/field, and 10 μM PLX4720 further reduced migration to

26 ± 6.7 cells/field ($p < .001$) (Fig. 3A, 3B). Invasion was also approximately twofold lower using 1 μM PLX4720 (27.2 ± 6.7 cells/field versus 52.7 ± 2.1 cells/field; $p < .001$) and fourfold lower using 10 μM (13.6 ± 4.0 cells/field versus 59.5 ± 8.8 cells/field; $p < .001$) (Fig. 3A, 3B).

PLX4720 CAUSES SIGNIFICANT REDUCTION IN CELL PROLIFERATION AND MIGRATION IN TPC-1 CELLS

TPC-1 is another authentic human thyroid carcinoma cell line [24] with a known *RET/PTC-1* translocation [27] that we have confirmed to have wt *B-Raf* and found to harbor a *PIK3CA* H1047R mutation (Fig. 1A) (by mass spectrometric genotyping); TPC-1 cells were found to be negative for other mutations (e.g., H-, N-, and K-*RAS* mutations, etc.). Though TPC-1 cells grew rapidly in vitro, they showed very low in vivo tumorigenicity, with a mean tumor size <1 mm^3 after 60 days post-orthotopic injection (supplemental online Fig. 2).

Paradoxically, in TPC-1 cells, treatment with 1 μM PLX4720 for 1 hour resulted in higher phospho-ERK-1/ERK-2 protein levels (by approximately 80%); however, 1 hour of treatment with 10 μM PLX4720 reduced phospho-ERK-1/ERK-2 by about 45% (Fig. 1B). Seventy-two hours of treatment with 1 μM or 10 μM PLX4720 resulted in persistently elevated levels of phospho-ERK-1/ERK-2 protein (95% and 400%, respectively) (Fig. 1B, 1C). Both 1 μM and 10 μM PLX4720 caused lower cell proliferation as measured by BrdU uptake ($27.9\% \pm 6.0\%$ in controls versus $12.9\% \pm 2.9\%$ with 1 μM PLX4720; $p = .01$ and $36.7\% \pm 2.2\%$ with control treatment versus $14.9\% \pm 0.2\%$ with 10 μM PLX4720; $p = .001$) (Fig. 2A–2C). Neither 1 μM nor 10 μM PLX4720 lead to apoptosis (absence of sub-G$_1$ cell population) in TPC-1 cells evaluated by flow cytometric analysis (Fig. 2D).

In addition, we found that only 10 μM PLX4720 reduced the migration of TPC-1 cells after 72 hours of treatment. Migration was about 1.6-fold lower (42.6 ± 16.7 cells/field versus 78.6 ± 6.8 cells/field) with 10 μM PLX4720 (Fig. 3A). No significant differences were found for invasion with either 1 μM or 10 μM PLX4720 (Fig. 3B). There was no significant difference in the levels of phospho-Akt ser473 (supplemental online Fig. 1A) or C-Raf with PLX4720, compared with controls (supplemental online Fig. 1B).

PLX4720 INHIBITS CELL PROLIFERATION, MIGRATION, AND INVASION IN NT CELLS WITH *B-RAF*^{V600E} OVEREXPRESSION

To understand the role of B-Raf^{V600E} in thyroid cell migration and invasion in the heterozygous setting, we stably overexpressed *B-Raf*^{V600E} in NT cells (passage 0). These NT cells have two wt *B-Raf* alleles, are positive for cytokeratin, and are negative for desmin, indicating epithelial origin. They are also positive for the following thyroid-specific markers: TSH receptor, thyroperoxidase (TPO), thyroid transcription factor (TTF)-1, and paired box gene 8 (PAX-8) (supplemental online Fig. 3). Stably overexpressing *B-Raf*^{V600E} in NT cells (*B-Raf*^{V600E}–NT cells) resulted in greater B-Raf mRNA and protein expression: 4.24 ± 0.1 copies in empty vector NT cells versus 52.4 ± 6.1 copies in *B-Raf*^{V600E}–NT cells ($p < .001$) (Fig. 3C). Stable *B-Raf*^{V600E} overexpression (detected by anti-tag-c-myc-B-Raf^{V600E} antibody) in these otherwise normal early-passage thyroid follicular cells, even in the presence of a wt *B-Raf* allele (heterozygous wt *B-Raf*/*B-Raf*^{V600E}), resulted in profound functional changes including: (a) significantly higher phospho-ERK-1/ERK-2 protein levels than in NT cells transduced with the empty vector (Fig. 3C), (b) greater cell migration (35.2 ± 5.2 cells/field in overexpressed *B-Raf*^{V600E} NT cells versus 6.7 ± 2.7 cells/field in the control; $p < .001$) (Fig. 3D), and (c) greater invasion (60.2 ± 8.0 cells/field in overexpressed *B-Raf*^{V600E} cells versus 12.2 ± 2.0 cells/field in the control; $p < .001$) (Fig. 3D).

PLX4720 treatment (1 μM) of *B-Raf*^{V600E}–NT cells resulted in lower migration—21.2 ± 7.4 cells/field versus 35.2 ± 5.2 cells/field in cells treated with the vehicle ($p < .05$)—and 10 μM was even more effective at reducing migration—10.7 ± 3.4 cells/field in cells treated with PLX4720 versus 37 ± 12.6 cells/field in cells treated with the vehicle; $p < .01$ (Fig. 3D). One micromolar PLX4720 also resulted in lower *B-Raf*^{V600E}–NT cell invasion—21 ± 0.8 cells/field versus 60.2 ± 8.0 cells/field in cells treated with the vehicle ($p < .001$). Ten micromolar PLX4720 was even more effective at reducing invasion—9.5 ± 1.9 cells/field in cells treated with PLX4720 versus 59 ± 11.1 cells/field in cells treated with the vehicle; $p < .001$ (Fig. 3D). *B-Raf*^{V600E}–NT cells treated with 10 μM PLX4720 (but not with 1 μM) showed significantly lower cell proliferation—$17.3\% \pm 1.8\%$ in cells treated with 10 μM PLX4720 versus $27.3\% \pm 0.7\%$ in cells treated with vehicle; $p = .01$ (supplemental online Fig. 4). No significant differences in cell proliferation (supplemental online Fig. 4), migration, or invasion were found in NT cells transduced with the empty vector treated with PLX4720 (either 1 μM or 10 μM), compared with the vehicle (Fig. 3D).

PLX4720 Inhibits Tumor Aggressiveness In Vivo

Sixteen animals had 8505c cells tagged with GFP orthotopically implanted into the right thyroid lobe. One week after tumor implantation, mice were randomized and treatment was initiated; eight animals were treated with PLX4720 (30
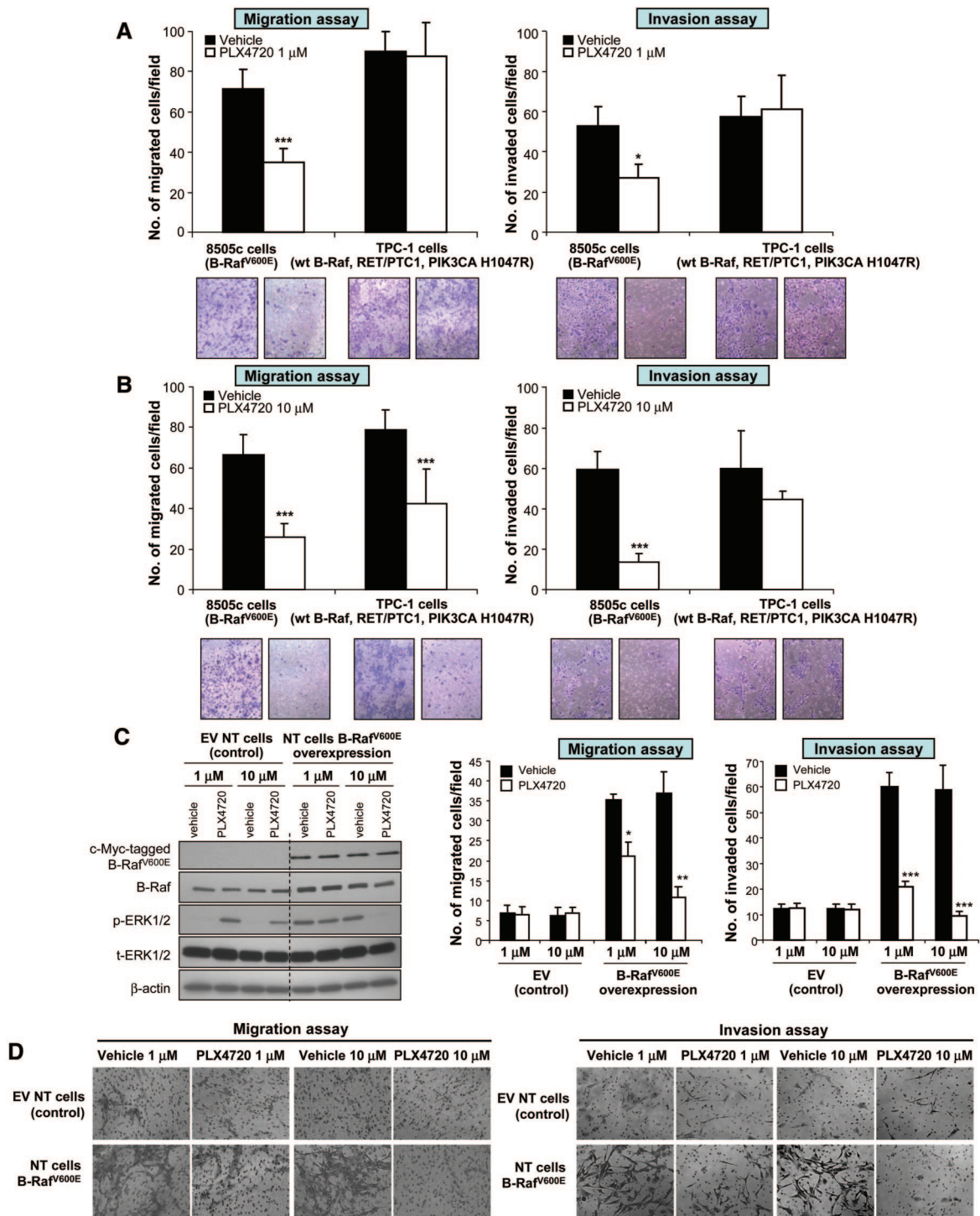
Figure 3. Migration and invasion assays with PLX4720 treatment in thyroid cancer cell models. Treatment with 1 μM **(A)** or 10 μM **(B)** PLX4720 reduced migration and invasion in 8505c cells (***$p < .001$). **(B):** Migration of TPC-1 cells was lower with 10 μM PLX4720 (***$p < .001$). **(C):** PLX4720 inhibited p-ERK-1/ERK-2 in *B-Raf*[V600E]-overexpressed primary human NT follicular cells, compared with NT cells transduced with the EV. **(D):** Migration and invasion of NT cells with *B-Raf*[V600E] overexpression were inhibited by PLX4720 (***$p < .001$).

Abbreviations: ERK, extracellular signal–related kinase; EV, empty vector; NT, normal thyroid; p, phosphorylated; wt, wild-type.

mg/kg per day for 21 days) by oral gavage and eight received control gavage. Control mice began to lose weight

and develop dramatic signs of cachexia at approximately 28 days. By 35 days, all controls showed evidence of cachexia

and demonstrated an average weight loss from baseline of 4.2 g $\pm$ 1.1 g (23% of baseline $\pm$ 6%) ($p < .001$) (Fig. 4). However, the mice in the PLX4720 treatment group maintained their weight and showed no signs of cachexia (Fig. 4). Five weeks post–tumor implantation, all animals were sacrificed and there was a dramatically (97%) lower tumor volume in PLX4720-treated animals than in controls (1.9 mm^3 versus 72 $\pm$ 18 mm^3; $p < .001$) (Fig. 4). These results confirm the in vivo effects of PLX4720 with thyroid cancer cells that harbor *B-Raf^{V600E}* [19]. Here, for the first time, we show detailed histological and IHC analyses performed on *B-Raf^{V600E}*-positive orthotopic thyroid carcinomas treated with PLX4720 or vehicle (control). The control tumors grew circumferentially around the trachea with extrathyroidal extension, and these tumors demonstrated histologic features of aggressiveness such as tracheal invasion, pleomorphism, and numerous mitotic figures (Fig. 5A1–5A4). The PLX4720-treated mice, however, had small and discrete tumor foci with minimal evidence of local invasion grossly or histologically (Fig. 5A5–5A8). Additionally, the proliferative index (Ki67 nuclear expression) in the PLX4720-treated orthotopic tumors was significantly lower than in the control ($p < .01$) (Fig. 4).

None of the mice showed gross evidence of lung metastasis, but on fluorescence microscopy there were numerous evident metastases in control mice lungs with a dramatically lower number of metastases in treated animals (99% lower) (Fig. 4B). Histologic evaluation showed that eight mice from the control group had multiple metastatic foci (average, 15.7 $\pm$ 2.4) (Fig. 5B1, 5B2), whereas no histological evidence of lung metastasis could be found in the lungs of the PLX4720-treated mice (average, 0) ($p < .001$) (Fig. 5B5, 5B6). Lymph node metastases are not frequently seen in our model of thyroid cancer (<50% of cases) (Fig. 5B3, 5B4) and no lymph node metastases were seen in the PLX4720-treated group (Fig. 5B7, 5B8).

Tumors from mice receiving PLX4720 showed upregulation of thyroid-specific cell differentiation markers (i.e., TTF-1 and PAX-8) at the protein level by IHC (Fig. 5C). IHC staining showed moderate immunoexpression of TTF-1 (diffuse nuclear localization) in PLX4720-treated 8505c orthotopic thyroid tumors, compared with weaker immunoexpression in untreated 8505c orthotopic thyroid tumors (control). Similarly, PAX-8 IHC showed weak cytoplasmic localization staining and absence in the nuclei in control orthotopic carcinomas, whereas the PLX4720-treated orthotopic carcinomas showed greater focal nuclear positivity (with normal thyroid follicular cells that were strongly positive in the nuclei) (Fig. 5C). Other thyroid cell differentiation markers, such as TPO, thyroglobulin (Tg), TSH receptor, and human sodium–iodide symporter

(hNIS), showed neither immunoexpression in the controls nor upregulation after 3 weeks of PLX4720 treatment in this model.

Additionally, given that PLX4720 caused a paradoxical increase in phospho-ERK-1/ERK-2 in vitro in wt *B-Raf* thyroid cancer cells (TPC-1) and wt *B-Raf* NT cells, we tested in vivo phospho-ERK-1/ERK-2 levels in mouse tissues that express wt *B-Raf* after treatment with PLX4720. We found no significant difference in phospho-ERK-1/ERK-2 levels in tissue protein extracts from muscles of SCID mice, compared with control animals, 35 days post–tumor injection (supplemental online Fig. 1B).

PLX4720 Downregulates Genes Involved in Cell Proliferation, Migration, and Invasion

In order to identify genes that are downstream targets of the B-Raf^{V600E} signaling cascade, we quantified absolute mRNA expression in vitro in both 8505c and TPC-1 human thyroid cancer cells following treatment with PLX4720 or vehicle. We analyzed mRNA copy number of early and late gene expression with 1 μM or 10 μM of PLX4720 for many genes crucial to the control of cell proliferation, migration, and invasion mechanisms (supplemental online Table 1).

In 8505c cells, we found that only high doses (10 μM) of PLX4720 led to significantly lower mRNA expression levels at 72 hours in the following: cyclin D1 (CCND1) (12.1 $\pm$ 0.4 copies), thrombospondin-1 (TSP-1) (12.6 $\pm$ 1.2 copies), and integrin α6 (ITGA6) (2.9 $\pm$ 0.33 copies), compared with controls (38.1 $\pm$ 1.7 copies, 45.6 $\pm$ 1.3 copies, and 9.7 $\pm$ 0.4 copies, respectively; $p < .05$) (Fig. 6).

In contrast, we found that the TSP-1 copy number was lower in 8505c cells after 24 hours of treatment with PLX4720 at both the 1 μM (32.4 $\pm$ 0.58 copies) and 10 μM (11.4 $\pm$ 0.9 copies) levels, compared with controls (67.84 $\pm$ 2.27 copies and 48.05 $\pm$ 0.9 copies, respectively; $p < .05$) (Fig. 6). In addition, the TSP-1 copy number was lower in TPC-1 cells treated with PLX4720 (at both the 1 μM and 10 μM levels) than in controls (Fig. 6).

In 8505c cells, we found that both 1 μM and 10 μM PLX4720 resulted in a higher mRNA expression level of the thyroid follicular cell differentiation marker TTF-1 at 72 hours of treatment (9.5 copies and 9.5 $\pm$ 0.4 copies, respectively) than in controls (5.1 $\pm$ 0.2 copies and 5.1 $\pm$ 0.3 copies, respectively; $p < .05$) (Fig. 6). The TTF-1 copy number was greater in 8505c cells after 24 hours of PLX4720 treatment with both 1 μM PLX4720 (25.5 $\pm$ 1.2 copies) and 10 μM PLX4720 (14.7 $\pm$ 0.3 copies) than in controls (19.6 $\pm$ 0.9 copies and 11.4 $\pm$ 0.5 copies, respectively; $p < .05$) (Fig. 6). In contrast, PAX-8 showed low mRNA basal levels (<1 copy number). Furthermore, TPO,
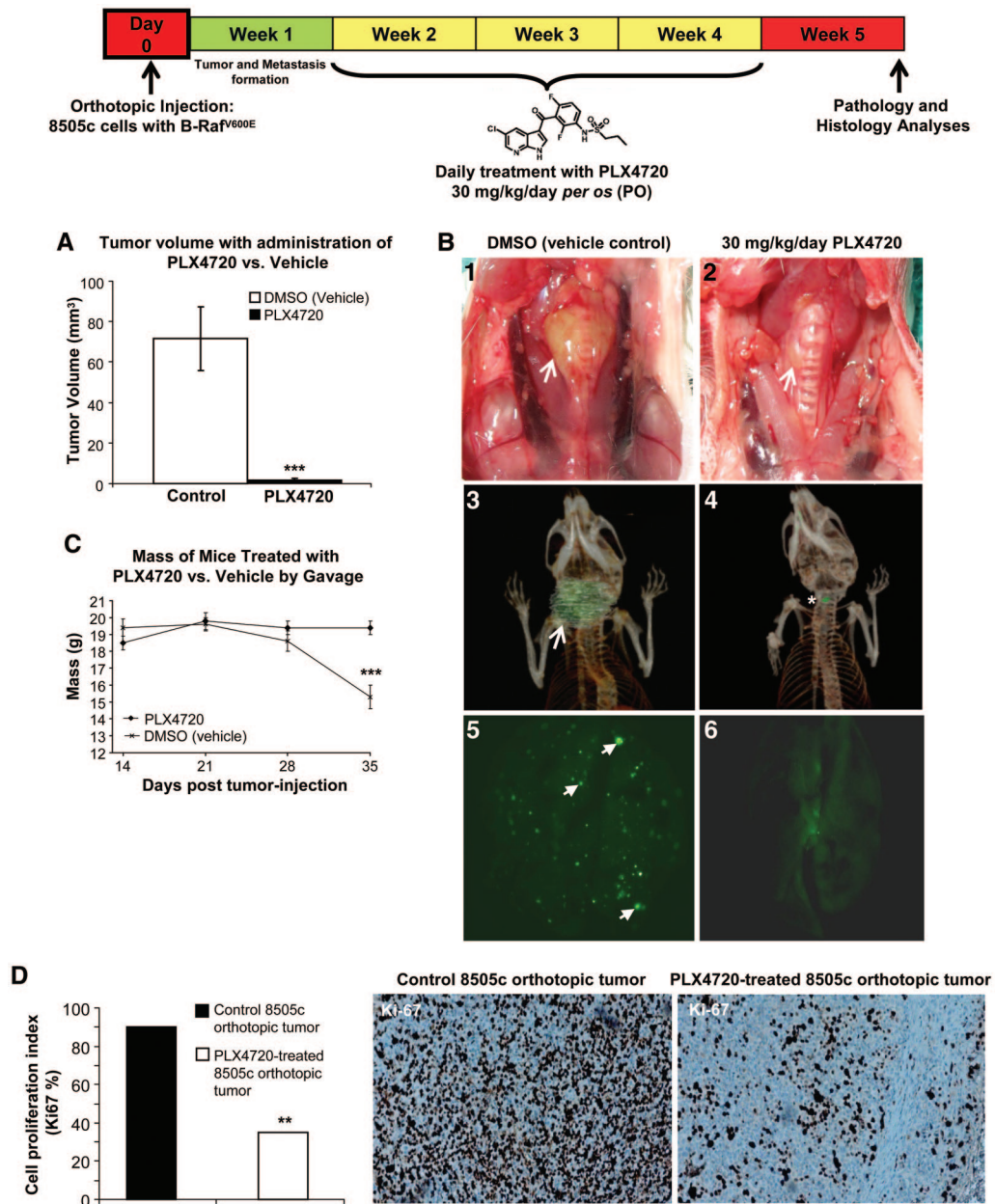
Figure 4. Tumor growth and lung metastasis in an orthotopic mouse model of human anaplastic thyroid cancer. **(A):** Three weeks of PLX4720 treatment resulted in lower orthotopic tumor growth than in controls (***p < .001). Gross photo **(B1)** and 3D CT scan **(B3)** show a large *B-Raf*[V600E] 8505c orthotopic thyroid carcinoma (control, arrow) and a dramatically smaller **(B2 and B4)** orthotopic tumor size with PLX4720 treatment (gross photo, arrow; 3D CT scans, asterisk) in SCID mice. **(B5):** Lung metastases (arrows) by GFP in control *B-Raf*[V600E] 8505c orthotopic thyroid carcinoma SCID mice. **(B6):** Significantly fewer lung metastases in PLX4720-treated mice. **(C)** Control mice became cachectic between 28 and 35 days and lost an average of 23% of their baseline weight, whereas PLX4720-treated mice maintained their baseline weight (***p < .001). **(D):** Low proliferative index (percentage of Ki-67 protein nuclear expression) in PLX4720-treated *B-Raf*[V600E] 8505c orthotopic tumors, compared with controls (**p < .01).

Abbreviations: 3D, three-dimensional; CT, computed tomography; DMSO, dimethyl sulfoxide; GFP, green fluorescent protein; SCID, severe combined immunodeficient.

Tg, TSH receptor, and hNIS showed very low mRNA copy numbers (<0.2 copy number) and no upregulation with PLX4720 treatment in 8505c cells; this result was also confirmed by IHC, which showed undetectable protein levels both in controls and in PLX4720-treated orthotopic thyroid carcinomas.
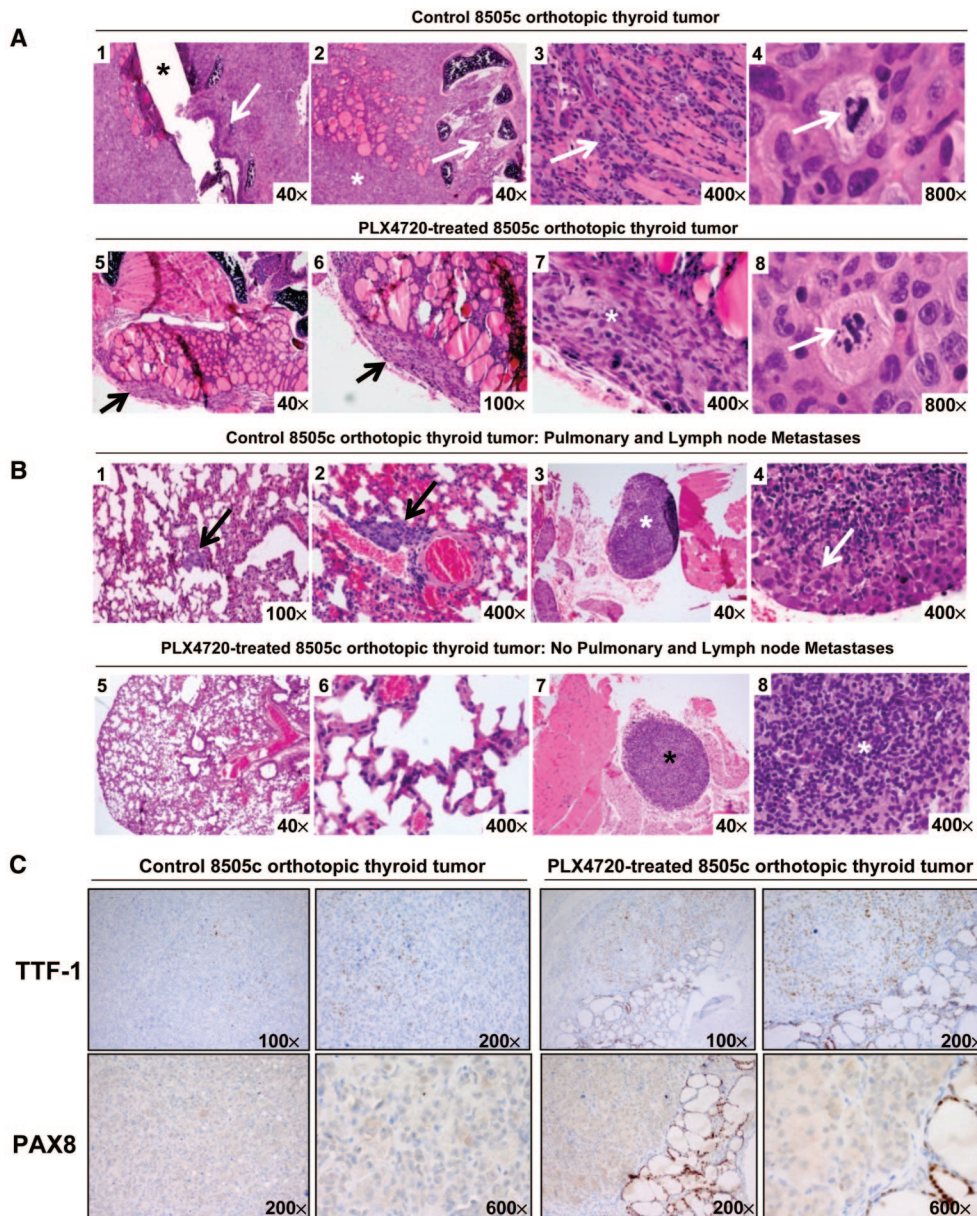
Figure 5. PLX4720 inhibits *B-Raf*^{V600E}-positive thyroid tumor aggressiveness in vivo. **(A):** Control mice with *B-Raf*^{V600E} 8505c orthotopic tumors (H&E stain) were large **(A1)** and showed extrathyroidal extension into the trachea **(A1, A2)** and skeletal muscle **(A3)** with atypical mitoses **(A4**, arrow); PLX4720-treated tumors (H&E stain) were small and discrete **(A5–A7)** (arrows) and largely confined to the thyroid bed, with atypical pyknotic nuclei **(A8)**. **(B):** Control SCID mice (H&E stain) had metastatic foci of carcinoma to the lung interstitium (arrows, **B1, B2**) as well as a paratracheal lymph node (asterisk, **(B3)**; higher power, arrow **(B4)**); PLX4720-treated mice had no evidence of metastasis to the lung **(B5, B6)** or lymph nodes **(B7, B8)**. **(C):** PLX4720-treated tumors had greater nuclear staining for TTF-1 and PAX-8 (right) than untreated control mice (left).

Abbreviations: H&E, hematoxylin and eosin; SCID, severe combined immunodeficient; TTF-1, thyroid transcription factor.

DISCUSSION

The typical treatment regimen of surgical excision, levo-thyroxine suppression, and radioactive iodine is successful in close to 90% of patients with differentiated thyroid cancer. However, for the group of patients who fail to respond to this treatment paradigm or initially present with aggressive and refractory thyroid carcinoma, survival rates are very low [28]. There are very few clinical trials for thyroid cancer [29], with a partial response rate of 30% in some single-agent studies [30]. The response rate for ATC is much lower, and consequently, >50% of thyroid cancer deaths are attributed to ATC [1].

By identifying the "driving events" behind thyroid cancer proliferation and migration/invasion, targeted molecu-
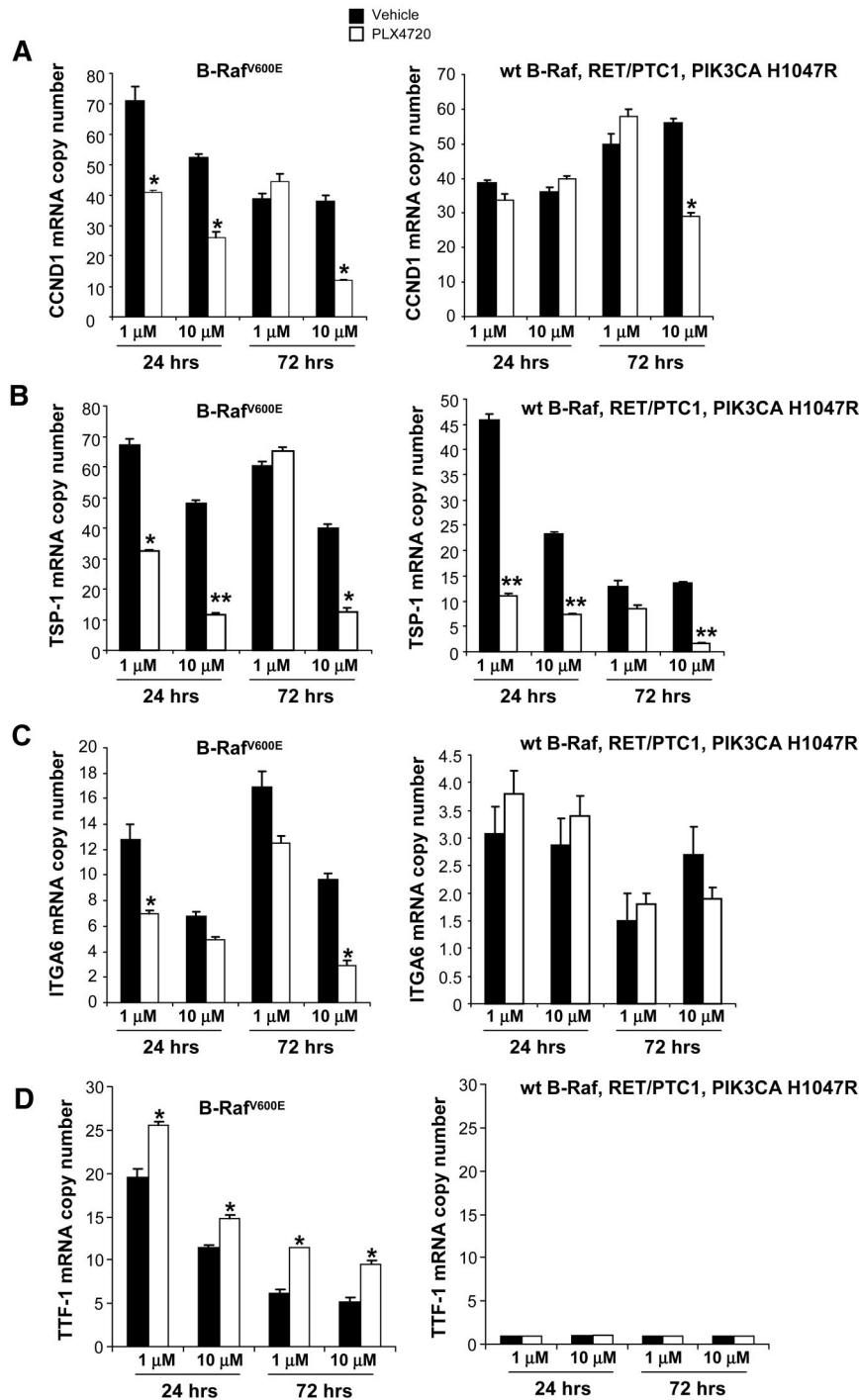
Figure 6. Gene expression with PLX4720 treatment. Quantitative real-time RT-PCR shows mRNA copy number of CCND1 (**A**), TSP-1 (**B**), ITGA6 (**C**), and TTF-1 (**D**) mRNA in 8505c and TPC-1 cells after 24 hours or 72 hours of treatment with PLX4720 (either 1 μM or 10 μM).

Abbreviations: CCND1, cyclin D1; ITGA6, integrin α6; RT-PCR, reverse transcriptase polymerase chain reaction; TSP-1, thrombospondin-1; TTF-1, thyroid transcription factor; wt, wild-type.

lar agents hold great potential for aggressive thyroid cancer. Current molecular strategies involve interrupting intracellular signal transduction pathways at specific targets, such as B-Raf, Ras, MEK, PI3K, RET, cMet, and epidermal growth factor [31]. Given that $B\text{-}Raf^{\text{V600E}}$ is the most prevalent mutation implicated in the initiation and aggressiveness of PTC, and possibly in the progression of PTC to ATC [31, 32], targeting this mutation holds great potential for

novel therapies. We chose to study this both in vitro and in vivo using PLX4720, a potent and selective B-Raf^{V600E} inhibitor. In one previous report, in vitro treatment of *B-Raf*^{V600E}-positive thyroid cancer cell lines with PLX4720 (50% inhibitory concentration in the range of 78–113 nM) showed cell cycle arrest, whereas *RET/PTC-1* and *Ras* mutated thyroid cancer cell lines were resistant to inhibition even at 500 nM [27].

In contrast, we found that only higher doses (both 1 μM and 10 μM) of PLX4720 caused cell cycle arrest and inhibited tumor cell migration and invasion in 8505c cells (*B-Raf*^{V600E}). Interestingly, by overexpressing *B-Raf*^{V600E} in NT cells, we were able to create a heterozygous model that genetically reproduces human thyroid cancers that have both a *B-Raf*^{V600E} allele and a wt *B-Raf* allele. With this overexpression of *B-Raf*^{V600E}, the ability of NT cells to invade and migrate was much greater than in controls. The gain of these functions was effectively inhibited by 10 μM PLX4720, suggesting a strong role for *B-Raf*^{V600E} in thyroid cancer progression. Therefore, this is the first in vitro translational demonstration that PLX4720 might be a useful compound in clinical trials for patients with thyroid cancers harboring the *B-Raf*^{V600E} mutation.

Recently, it was shown that PLX4720 could have unexpected effects in some cell contexts (e.g., presence of wt *B-Raf* and mutated *Ras*) as a result of ERK-1/ERK-2 activation [25, 33, 34]. However, in our study, PLX4720 treatment of NT cells (wt *B-Raf*/wt *B-Raf*) transduced with empty vector did not result in greater proliferation, migration, or invasion despite a higher level of phospho-ERK-1/ERK-2. Somewhat unexpectedly, cell proliferation and migration were also inhibited in TPC-1 cells (*RET/PTC-1* translocation, *PIK3CA* H1047R mutation, and wt *B-Raf*). These results indicate that certain wt *B-Raf* thyroid tumors (perhaps those that harbor *RET/PTC-1* and/or *PIK3CA* H1047R) might be somewhat responsive to PLX4720 treatment as well. Further preclinical validation is needed to understand this phenomenon prior to human testing.

PLX4720 treatment downregulated genes involved in cell proliferation, such as *CCND1*, and certain genes known to be important in migration, invasion, and metastasis, such as *TSP-1* and *ITGA6* [35]. We have previously shown that knockdown of *TSP-1* decreases phospho-ERK-1/ERK-2 levels and reduces thyroid cancer progression [19], perhaps through binding of the N-terminal domain of TSP-1 to integrins such as $\alpha3\beta1$ or $\alpha6\beta1$ [36, 37]. TSP-1 is known to be intimately involved in the regulation of cellular proliferation by affecting early response genes [38], and our data are consistent with those results [19].

Our in vitro studies show higher phospho-ERK-1/ERK-2 levels when TPC-1 cells are treated with PLX4720.

Recent findings by Hatzivassiliou et al. [34] showed that ATP-competitive Raf inhibitors, including PLX4720, have opposing roles as inhibitors and activators of ERK-1/ERK-2 phosphorylation depending on the cellular and genotypic context. Furthermore, other authors recently reported that inhibition of wt *B-Raf* by PLX4720 in *Ras* mutant (e.g., N-*Ras*) human cancer cells (i.e., melanoma cells) leads to MEK–ERK-1/ERK-2 hyperactivation through C-Raf [25]. These aforementioned studies [25, 33, 34, 39] and others [40] highlight the importance of individualized genomic profiling to guide patient selection for inclusion in targeted therapy trials. We also found that PLX4720 treatment in vitro and in vivo in 8505c cells upregulated important thyroid-related transcription factors, such as TTF-1 and PAX-8, that have been widely described as markers of thyroid follicular cell differentiation, thus suggesting that *B-Raf*^{V600E} might play a biological role in thyroid follicular cell dedifferentiation.

In vivo, we demonstrated a dramatic reduction in tumor aggressiveness in our orthotopic mouse model of ATC. PLX4720 treatment reduced tumor volume by 97% and virtually eliminated metastatic spread to the lungs. Though the ATC cell line 8505c also harbors a *TP53* mutation [41], the selective inhibition of *B-Raf*^{V600E} was sufficient to dramatically reduce tumor volume, extrathyroidal extension, and metastasis without any obvious toxicity. Both in vitro and in vivo results point to the potential therapeutic utility of this drug in patients with advanced *B-Raf*^{V600E} thyroid cancers.

In conclusion, our study shows that inhibition of *B-Raf*^{V600E} with the novel agent PLX4720 results in dramatic changes in cell proliferation, migration, and invasion in vitro, and early intervention with this drug results in marked inhibition of tumor aggressiveness in an in vivo model of ATC harboring *B-Raf*^{V600E}. Our in vitro model using primary human NT follicular cells (heterozygous wt *B-Raf*/*B-Raf*^{V600E}) recapitulates the genetic status of this mutation in human thyroid cancer, and is the first preclinical model to show that PLX4720 inhibits cell proliferation, migration, and invasion in a *B-Raf*^{V600E} heterozygous model. PLX4720 might be an effective therapy for appropriately selected patients with metastatic or refractory thyroid cancers that harbor the *B-Raf*^{V600E} mutation.

SUMMARY AND CLINICAL RELEVANCE

Despite considerable enthusiasm about targeted therapies and understanding the underlying reasons why the *B-Raf*^{V600E} mutation may lead to more aggressive clinical behavior in some patients with thyroid cancer, there have not been many studies on the inhibition of *B-Raf*^{V600E}. Our study shows that inhibition of *B-Raf*^{V600E} with the novel agent PLX4720 can decrease cell proliferation, migration, and invasion in thyroid cancer cell lines and markedly in-

hibit tumor growth and metastasis in an orthotopic mouse model of human ATC harboring *B-Raf*^{V600E}. Additionally, our in vitro model using primary human NT cells (heterozygous wt *B-Raf/B-Raf*^{V600E}) recapitulates the genetic status of this mutation in human thyroid cancer; it is the first translational demonstration to show that PLX4720 is effective in a *B-Raf*^{V600E} heterozygous model. Our results suggest that PLX4720 might be an effective therapy in clinical trials for the treatment of patients with *B-Raf*^{V600E}-positive thyroid cancers that are refractory to conventional therapy.

Author Contributions

Conception/Design: Carmelo Nucera, Matthew A. Nehs, Sareh Parangi
Provision of study material or patients: Carmelo Nucera, Matthew A. Nehs, Peter M. Sadow, Paul S. Lin, Gideon E. Bollag, Jack Lawler, Sareh Parangi
Collection and/or assembly of data: Carmelo Nucera, Matthew A. Nehs, Sushruta S. Nagarkatti, Peter M. Sadow, Michal Mekel, Andrew H. Fischer
Data analysis and interpretation: Carmelo Nucera, Matthew A. Nehs, Jack Lawler, Richard A. Hodin, Sareh Parangi
Manuscript writing: Carmelo Nucera, Matthew A. Nehs
Final approval of manuscript: Carmelo Nucera, Matthew A. Nehs, Sushruta S. Nagarkatti, Peter M. Sadow, Michal Mekel, Andrew H. Fischer, Paul S. Lin, Gideon E. Bollag, Jack Lawler, Richard A. Hodin, Sareh Parangi

References

1 National Comprehensive Cancer Network. NCCN Clinical Practice Guidelines in Oncology 2007. Available at http://www.nccn.org/professionals/physician_gls/f_guidelines.asp, accessed September 2009.

2 Pacini F. Where do we stand with targeted therapy of refractory thyroid cancer?—utility of RECIST criteria. Thyroid 2008;18:279–280.

3 Ciampi R, Nikiforov YE. RET/PTC rearrangements and BRAF mutations in thyroid tumorigenesis. Endocrinology 2007;148:936–941.

4 Santoro M, Melillo RM, Carlomagno F et al. Molecular mechanisms of RET activation in human cancer. Ann N Y Acad Sci 2002;963:116–121.

5 Giordano TJ, Kuick R, Thomas DG et al. Molecular classification of papillary thyroid carcinoma: Distinct BRAF, RAS, and RET/PTC mutation-specific gene expression profiles discovered by DNA microarray analysis. Oncogene 2005;24:6646–6656.

6 Xing M. BRAF mutation in thyroid cancer. Endocr Relat Cancer 2005;12:245–262.

7 Frasca F, Nucera C, Pellegriti G et al. BRAF(V600E) mutation and the biology of papillary thyroid cancer. Endocr Relat Cancer 2008;15:191–205.

8 Davies H, Bignell GR, Cox C et al. Mutations of the BRAF gene in human cancer. Nature 2002;417:949–954.

9 Emuss V, Garnett M, Mason C et al. Mutations of C-RAF are rare in human cancer because C-RAF has a low basal kinase activity compared with B-RAF. Cancer Res 2005;65:9719–9726.

10 Wan PT, Garnett MJ, Roe SM et al. Mechanism of activation of the RAF-ERK signaling pathway by oncogenic mutations of B-RAF. Cell 2004;116:855–867.

11 Knauf JA, Fagin JA. Role of MAPK pathway oncoproteins in thyroid cancer pathogenesis and as drug targets. Curr Opin Cell Biol 2009;21:296–303.

12 Mitsutake N, Knauf JA, Mitsutake S et al. Conditional BRAFV600E expression induces DNA synthesis, apoptosis, dedifferentiation, and chromosomal instability in thyroid PCCL3 cells. Cancer Res 2005;65:2465–2473.

13 Begum S, Rosenbaum E, Henrique R et al. BRAF mutations in anaplastic thyroid carcinoma: Implications for tumor origin, diagnosis and treatment. Mod Pathol 2004;17:1359–1363.

14 Tsai J, Lee JT, Wang W et al. Discovery of a selective inhibitor of oncogenic B-Raf kinase with potent antimelanoma activity. Proc Natl Acad Sci U S A 2008;105:3041–3046.

15 Meireles AM, Preto A, Rocha AS et al. Molecular and genotypic characterization of human thyroid follicular cell carcinoma-derived cell lines. Thyroid 2007;17:707–715.

16 Fischer AH, Taysavang P, Jhiang SM. Nuclear envelope irregularity is induced by RET/PTC during interphase. Am J Pathol 2003;163:1091–1100.

17 Boehm JS, Zhao JJ, Yao J et al. Integrative genomic approaches identify IKBKE as a breast cancer oncogene. Cell 2007;129:1065–1079.

18 Nucera C, Eeckhoute J, Finn S et al. FOXA1 is a potential oncogene in anaplastic thyroid carcinoma. Clin Cancer Res 2009;15:3680–3689.

19 Nucera C, Porrello A, Antonello ZA et al. B-Raf(V600E) and thrombospondin-1 promote thyroid cancer progression. Proc Natl Acad Sci U S A 2010;107:10649–10654.

20 Shih SC, Smith LE. Quantitative multi-gene transcriptional profiling using real-time PCR with a master template. Exp Mol Pathol 2005;79:14–22.

21 Nucera C, Nehs MA, Mekel M et al. A novel orthotopic mouse model of human anaplastic thyroid carcinoma. Thyroid 2009;19:1077–1084.

22 Ji H, Wang Z, Perera SA et al. Mutations in BRAF and KRAS converge on activation of the mitogen-activated protein kinase pathway in lung cancer mouse models. Cancer Res 2007;67:4933–4939.

23 Puxeddu E, Moretti S, Giannico A et al. Ret/PTC activation does not influence clinical and pathological features of adult papillary thyroid carcinomas. Eur J Endocrinol 2003;148:505–513.

24 Schweppe RE, Klopper JP, Korch C et al. Deoxyribonucleic acid profiling analysis of 40 human thyroid cancer cell lines reveals cross-contamination resulting in cell line redundancy and misidentification. J Clin Endocrinol Metab 2008;93:4331–4341.

25 Heidorn SJ, Milagre C, Whittaker S et al. Kinase-dead BRAF and onco-

genic RAS cooperate to drive tumor progression through CRAF. Cell 2010; 140:209–221.

26 Shaw RJ, Cantley LC. Ras, PI(3)K and mTOR signalling controls tumour cell growth. Nature 2006;441:424–430.

27 Salerno P, De Falco V, Tamburrino A et al. Cytostatic activity of adenosine triphosphate-competitive kinase inhibitors in BRAF mutant thyroid carcinoma cells. J Clin Endocrinol Metab 2010;95:450–455.

28 Sherman SI. Advances in chemotherapy of differentiated epithelial and medullary thyroid cancers. J Clin Endocrinol Metab 2009;94:1493–1499.

29 Tuttle RM, Leboeuf R. Investigational therapies for metastatic thyroid carcinoma. J Natl Compr Canc Netw 2007;5:641–646.

30 Sherman SI. Tyrosine kinase inhibitors and the thyroid. Best Pract Res Clin Endocrinol Metab 2009;23:713–722.

31 Xing M. BRAF mutation in papillary thyroid cancer: Pathogenic role, molecular bases, and clinical implications. Endocr Rev 2007;28:742–762.

32 Nucera C, Goldfarb M, Hodin R et al. Role of B-Raf(V600E) in differentiated thyroid cancer and preclinical validation of compounds against B-Raf(V600E). Biochim Biophys Acta 2009;1795:152–161.

33 Poulikakos PI, Zhang C, Bollag G et al. RAF inhibitors transactivate RAF dimers and ERK signalling in cells with wild-type BRAF. Nature 2010;464: 427–430.

34 Hatzivassiliou G, Song K, Yen I et al. RAF inhibitors prime wild-type RAF to activate the MAPK pathway and enhance growth. Nature 2010;464:431–435.

35 Patel MK, Lymn JS, Clunn GF et al. Thrombospondin-1 is a potent mitogen and chemoattractant for human vascular smooth muscle cells. Arterioscler Thromb Vasc Biol 1997;17:2107–2114.

36 Chandrasekaran S, Guo NH, Rodrigues RG et al. Pro-adhesive and chemotactic activities of thrombospondin-1 for breast carcinoma cells are mediated by $\alpha 3 \beta 1$ integrin and regulated by insulin-like growth factor-1 and CD98. J Biol Chem 1999;274:11408–11416.

37 Iyer V, Pumiglia K, DiPersio CM. $\alpha 3 \beta 1$ integrin regulates MMP-9 mRNA stability in immortalized keratinocytes: A novel mechanism of integrin-mediated MMP gene expression. J Cell Sci 2005;118:1185–1195.

38 Majack RA, Mildbrandt J, Dixit VM. Induction of thrombospondin messenger RNA levels occurs as an immediate primary response to platelet-derived growth factor. J Biol Chem 1987;262:8821–8825.

39 Kwong LN, Chin L. The brothers RAF. Cell 2010;140:180–182.

40 Emery CM, Vijayendran KG, Zipser MC et al. MEK1 mutations confer resistance to MEK and B-RAF inhibition. Proc Natl Acad Sci U S A 2009; 106:20411–20416.

41 Yoshimoto K, Iwahana H, Fukuda A et al. Role of p53 mutations in endocrine tumorigenesis: Mutation detection by polymerase chain reaction-single strand conformation polymorphism. Cancer Res 1992;52:5061–5064.